HHS Public Access

Author manuscript

Mol Cancer Ther. Author manuscript; available in PMC 2018 October 01.

Published in final edited form as:

Mol Cancer Ther. 2017 October ; 16(10): 2201–2214. doi:10.1158/1535-7163.MCT-16-0924.

Epidermal Growth Factor Receptor (EGFR) Targeted Photoimmunotherapy (PIT) for the Treatment of EGFR expressing Bladder Cancer

Reema Railkar[1], **L. Spencer Krane**[1], **Q. Quentin Li**[1], **Thomas Sanford**[1], **Mohammad Rashid Siddiqui**[1], **Diana Haines**[2], **Srinivas Vourganti**[1,*], **Sam J. Brancato**[1,#], **Peter L. Choyke**[3], **Hisataka Kobayashi**[3], and **Piyush K. Agarwal**[1]

[1]Urologic Oncology Branch, Center for Cancer Research, National Cancer Institute, Bethesda, MD -20892

[2]Pathology Section, Pathology/Histotechnology Laboratory, Leidos Biomedical Research, Inc. Frederick National Laboratory for Cancer Research, Frederick, MD 21702

[3]Molecular Imaging Program, Center for Cancer Research, National Cancer Institute, Bethesda, MD -20892

Abstract

The use of light as a means of therapy for bladder cancer (BC) has a long history but has been hampered by a lack of tumor specificity and therefore, damage to the normal bladder mucosa. Here, we describe a targeted form of photo-therapy called photoimmunotherapy (PIT) which targets EGFR-expressing BC. Anti-EGFR antibody panitumumab (pan) was labeled with the photo-absorber (PA), IRDye 700Dx (IR700), to create a pan IR700 antibody-PA conjugate which is activated by near-infrared radiation (NIR). BC tissue microarray (TMA) and BC cell lines were analyzed for expression of EGFR. Mechanism of PIT induced cell death was studied using proliferation assays, transmission electron microscopy (TEM), and production of reactive oxygen species. Finally, the in vivo effect was studied in xenografts. EGFR staining of TMAs showed that while most BCs have expression of EGFR to a varying degree, squamous cell carcinomas (SCC) have the highest expression of EGFR. Pan IR700 activated by NIR light rapidly killed UMUC-5 cells, a bladder SCC line. Pan alone, pan IR700 without NIR, or NIR alone had no effect on cells. TEM demonstrated that cell death is due to necrosis. Singlet oxygen species contributed towards cell death. NIR-PIT with pan IR700 reduced growth compared to only pan IR700 treated UMUC-5 xenograft tumors. PIT is a new targeted treatment for bladder cancer. Pan IR700-induced PIT selectively kills EGFR-expressing BC cells in vitro and in vivo and therefore warrants further therapeutic studies in orthotopic xenografts of BC and ultimately in patients.

Corresponding Author – Piyush K. Agarwal, Urologic Oncology Branch, Building 10 - Hatfield CRC, Room 2-5940, Bethesda, MD 20892-1210, Phone No. 301-496-6353, piyush.agarwal@nih.gov.

*Department of Urology, Rush University Medical Center

#Department of Urology, University of Iowa, Iowa City, IA 52242

Keywords

immunoconjugate; photoimmunotherapy; photodynamic therapy; urothelial cancer; bladder cancer; anti-EGFR

Introduction

Bladder cancer (BC) is the fourth most common cancer in men and the 12th most common cancer in women. There will be an estimated 76,960 new cases and 16,390 deaths attributed to bladder cancer in 2016 (ranking 8th in all cancer related deaths in men) (1). In addition to its prevalence, BC is the most expensive malignancy to treat from diagnosis to death (2). Unfortunately, the standard of care for localized BC treatment has undergone only incremental improvement over the past several decades. Approximately 70% of cases are non-muscle invasive bladder cancer (NMIBC) at presentation and are treated by transurethral resection of bladder tumor (TURBT) followed by intravesical treatment with BCG (Bacillus Calmette-Guerin) or mitomycin C. However, in the setting of high grade disease, these therapies can become ineffective over time in up to two-thirds of patients (3) and disease progression to muscle invasive bladder cancer (MIBC) can occur. MIBC is aggressive and only 50% of patients will survive five years despite undergoing radical cystectomy (4). Clearly, there is a large unmet need in therapeutic options for NMIBC that recurs or progresses.

A potential therapeutic target is the epidermal growth factor receptor (EGFR). EGFR is overexpressed in up to 74% of bladder cancer tissue specimens(5) but has a relatively low expression in normal urothelium (6). In addition, EGFR is an independent predictor of decreased survival and stage progression in bladder cancer (5). The Cancer Genome Atlas (TCGA) project revealed EGFR amplification in up to 11% of MIBC with predominant urothelial cell carcinoma histology (UCC) (7). EGFR is localized to the basal layer of urothelial cells in normal urothelium but is present in both the luminal and basal layers of urothelial cells in bladder cancer (8). This amplification and luminal localization of EGFR in urothelial tumors make intravesical therapy a potential treatment option in bladder cancer. EGFR is especially amplified in squamous cell carcinomas (SCC) of the bladder. Only 2–5% of all BC cases are pure squamous cell carcinoma (SCC) of the bladder (9), however, up to 60% of UCC contain histologic features of squamous differentiation (10). Previous immunohistochemical observations demonstrate that about 67% of bladder cancers with squamous differentiation express EGFR (11) and about 90% of pure SCCs of bladder express EGFR (12,13). Therefore, EGFR appears to be a viable target in all pure SCC, most UCC with squamous differentiation, and some UCC without squamous differentiation.

In the present study, we targeted EGFR-expressing BC cells using the anti-EGFR antibody panitumumab (pan) conjugated with IR700, a photosensitizer (PS) / photo-absorber (PA). IR700 is a highly hydrophilic dye activated by near infrared radiation (NIR) of ~689nm. By itself, it has no therapeutic effect as its hydrophilic nature prevents it from interacting with cell membranes, thereby decreasing toxicity. However, the pan IR700 conjugate selectively binds to EGFR-expressing cells and, when activated with NIR, selectively destroys only

cells bound to the conjugate. Unlike traditional photosensitizers, pan IR700 is more selective with fewer potential side effects. This novel use of a monoclonal antibody-photo-absorber conjugate has been termed “photoimmunotherapy” (PIT) (14). We detail our pre-clinical study of the efficacy and mechanism of action of PIT in bladder cancer cell lines using the pan IR700 immunoconjugate as a novel and selective therapeutic strategy for bladder cancer.

Materials and Methods

Chemicals and Reagents

The water soluble phthalocyanine dye IRDye 700DX NHS ester was purchased from LI-COR Bioscience. A fully human monoclonal antibody (mAb) against human Epidermal Growth Factor Receptor (hEGFR), panitumumab, was procured from Amgen (Thousand Oaks, CA). Rat mAb against hEGFR conjugated with Phycoerithrin (PE), PE conjugated Rat IgG2a, and kappa mAb (isotype control) were obtained from Abcam (Cambridge, MA). All other chemicals were reagent grade.

Synthesis of IR700 Conjugated Panitumumab (Pan IR700)

Panitumumab was conjugated with IRDye 700Dx NHS ester according to a previously published protocol(14). The conjugated antibody was purified using Sephadex G50 column (PD-10 from GE Healthcare). The antibody concentration was determined by measuring the absorption at 280 nm (8453 Value System; Agilent Technologies). Similarly, the amount of IR700 conjugated was determined by absorption at 689nm. The synthesis of pan IR700 was controlled such that each antibody molecule bound on average three to four IR700 molecules. The purity of pan IR700 was assessed using SDS-PAGE. The fluorescent band of pan IR700 was measured using Odyssey Infrared Imager (LI-COR) at 700nm.

Cell Culture

The bladder cancer cell lines TCCSUP (HTB-5), 5637 (HTB-9), RT4 (HTB-2), T24 (HTB-4), ScaBER (HTB-3), HT1197 (CRL-1473), HT1376 (CRL-1472), UMUC-3 (CRL-1749), SW780 (CRL-2169), epidermoid carcinoma cell line A431 (CRL-1555) and breast cancer cell line MDA-MB-453 (HTB-131) were obtained from ATCC (Manassas, VA, USA). RT112 was obtained from DSMZ, Germany. Metastatic lines of T24 and UMUC-3, T24T, FL3, SLT3 and Lul-2 were gifted by Dr. Michael Nickerson (Division of Cancer Epidemiology & Genetics, NCI). MGH-U3 was obtained from Massachusetts General Hospital. The bladder cancer cell line UMUC-5 was a kind gift of Dr. David McConkey (University of Texas, MD Anderson Cancer Center). UOBL103 is a human SCC cell line established within our laboratory. The normal urothelial cell line, UPS 54, was a kind gift from Dr. Toby Chai (Yale University). All the cells except MDA-MB-453 and UPS54 were grown in minimum essential media (MEM) (Life Technologies) supplemented with 10% fetal bovine serum, 1% penicillin/streptomycin and 1% GlutaMAX (Life Technologies). For UPS54, this medium was supplemented with insulin (1U/ml) and amphotericin B (1.25μg/ml). MDA-MB-453 was grown in RPMI 1640 (Life Technologies) instead. All cells required humidified incubator at 37°C with 5% CO_2 for growth. The cell lines were authenticated using STR analysis by Protein Expression Laboratory Core facility of Frederick National Laboratory for Cancer Research (FNLCR). The STR multiplex assay amplifies both 15

tetranucleotide repeat loci and the Amelogenin gender determination marker in a single PCR amplification. Large number of freezes were prepared from each authenticated cell line and once thawed, the cells were used only for 5–8 passages to maintain the integrity of cells.

Flow Cytometry

The presence of EGFR on the surface of bladder cancer cell lines was determined by flow cytometry. Single cell suspension of these cells (~ 1×10^6 cells/tube) was incubated in the presence of PE-tagged Rat mAb to hEGFR (Abcam) or PE-tagged Rat IgG2a, kappa mAb (isotype control; Abcam) for 30 minutes at 4 °C. Unbound antibody was then washed off and fluorescence was measured on FACS Calibur flow cytometer (BD BioSciences) and data was analyzed on software FlowJo (Treestar Inc.). A431 and MDA-MB-453 were used as positive and negative controls, respectively, for the expression of EGFR.

In Vitro Photoimmunotherapy (PIT)

The bladder cancer cells were plated in 35mm dishes or 96-well plates for 24 hours. The medium was replaced by fresh, phenol-free media containing no drug, pan, pan IR700, or IR700 for 1 hour at 37°C. The cells were then irradiated with 4–100 J/cm^2 NIR (670–710 nm). Unless otherwise stated, most of the following assays were carried out 20–30 minutes post NIR irradiation.

LIVE/DEAD Cytotoxicity Assay

The cytotoxic effect of pan IR700 based PIT was tested on UMUC-5 and 5637 cells. The PIT treated cells (pan IR700 10μg/ml + 4 J/cm^2 NIR for UMUC-5 and 32 J/cm^2 for 5637) were trypsinized and washed with PBS. One microliter/tube of LIVE/DEAD reagent (Life Technologies) was added to cell suspension. Following the incubation at 18–25°C for 30 minutes, cells were analyzed on a flow cytometer.

MTS Cell Proliferation Assay (Promega)

About 20,000 cells/well were seeded in a 96-well plate and incubated for 24 hours, followed by addition of increasing concentrations of pan/pan IR700. After incubation at 37°C for 1 hour, the cells were exposed to NIR and kept in dark at 37°C for 24 hours. Twenty microliters of MTS reagent were added to each well and plates were kept again in dark for an additional 2–3 hours. The optical density was measured at 490 nm. The half maximal inhibitory concentration (IC_{50}) values were calculated using GraphPad Prism version 6.01 (GraphPad Software; La Jolla, CA, USA) software.

FITC Annexin V – DNA Binding Dye (FxCycle™ Violet) Assay

Single cell suspensions (1×10^6 cells/tube) were prepared from PIT treated cells and incubated with FITC annexin V (BioLegend, San Diego, CA, USA) and FxCycle™ Violet (Molecular Probes, Life Technologies) solutions for 15 minutes in dark at room temperature. The type of cell death was evaluated on a flow cytometer using appropriate gates and quadrants.

Caspase-Glo 3/7 Assay

About 10000 cells/well of UMUC-5, 5637, and UMUC-3 cell lines were incubated overnight in white walled, clear bottom 96-well plates. The apoptosis inducer, Staurosporine (1μM) (SelleckChem) (PubChem CID – 44259), was incubated with the cells for 3–4 hours in the presence and absence of the caspase inhibitor Z-VAD-FMK (20μM) (Promega Corporation) (PubChem CID – 5497174). Experimental wells were treated with 10μg/ml of pan/pan IR700 or an equivalent concentration of IR700 with or without Z-VAD-FMK (20μM) for 1 hour followed by irradiation with an appropriate amount of NIR (UMUC-5 – 4 J/cm^2, 5637 – 32 J/cm^2 and UMUC-3 – 64 J/cm^2). Approximately 20 to 30 minutes post-NIR treatment, 100μl of Caspase-Glo 3/7 reagent was added to each well. Plates were incubated at room temperature for 30 minutes and luminescence was measured using EnSpire multimode plate reader (Perkin Elmer).

Transmission Electron Microscopy (TEM)

PIT treated cells were trypsinized and fixed overnight in 2.5% glutaraldehyde in 0.1 M Cacodylate buffer, pH 7.4. This was followed by secondary fixation in 1% osmium tetroxide in 0.1 M cacodylate buffer, pH 7.4, dehydration in increasing strength of ethanol, and finally infiltration and embedding in resin. Images for cellular ultra-structure were obtained by thin section TEM.

2',7'-Dichlorofluorescein Diacetate (DCFDA) Assay (Abcam) for the Measurement of Reactive Oxygen Species (ROS)

About 25000 cells/well were incubated overnight in black walled, clear bottom 96-well plates. The cells were washed in assay buffer and stained with 20μM DCFDA prepared in assay buffer for 45 minutes at 37°C in the dark. DCFDA was washed off using assay buffer and cells were incubated with pan/pan IR700/IR700 in the presence or absence of water soluble anti-oxidant Trolox (1 mM). The fluorescent signal pre- and post-NIR exposure was measured on VICTOR^{3}V Multi-label counter (Perkin Elmer) using fluorescein filter (Ex. 485 nm/Em. 535 nm).

Singlet Oxygen Sensor Green (SOSG) Assay for the Detection of Singlet Oxygen Species (SOS)

SOSG reagent (Molecular Probes, Life Technologies) was used to detect the presence of singlet oxygen in PIT treated cells. The assay protocol is similar to the DCFDA assay above except a known inhibitor of singlet oxygen generation, NaN_3 (10 mM), was used instead of Trolox.

In Vivo Photoimmunotherapy (PIT)

Three million UMUC-5 cells resuspended in 50% Matrigel or 3 million UMUC-3 cells were injected subcutaneously on the right thigh of female Athymic Nu/Nu mice (Charles River Laboratory, Frederick National Laboratory, Frederick, MD) of 6–8 weeks of age. All *in vivo* procedures were conducted in compliance with the Guide for Care and Use of Laboratory Animal Resources (1996), U.S. National Research Council, and approved by the local Animal Care and Use Committee. Volume of each tumor was determined using an external

caliper. The tumor volumes were calculated using the following formula: Tumor volume = Tumor length × Tumor width^2 × 0.5. When the tumor volumes reached ~ 50 mm^3, the mice were randomized in two groups of 10 mice each for the following treatment – Control group: 120 μg pan IR700 injected intravenously without NIR and Experimental group: 120 μg pan IR700 injected intravenously followed by 2 doses of NIR, 100 J/cm^2 and 50 J/cm^2, 24 and 48 hours after pan IR700 injection, respectively. The mice were anesthetized using 3% isoflurane and were kept asleep throughout the period of NIR exposure. After treatment, the mice were monitored periodically and tumors were measured twice per week. When the UMUC-5 tumors reached 500–1000 mm^3, the mice were euthanized using CO_2. The tumors were dissected out, weighed and fixed immediately in 10% buffered formalin. Mice bearing rapidly growing UMUC-3 tumors were euthanized when tumor size reached 20mm in any dimension.

Immunohistochemistry (IHC) Analysis

Paraffin blocks were prepared from fixed tumors. Four μm sections were cut on slides from these blocks and stained for haematoxylin and eosin (H&E) to detect the percentage of necrotic cells in tumors treated with/without PIT. These tumor sections were also analyzed for presence of hEGFR using anti-hEGFR antibody (Cell Signaling Technology No. 4267). In short, slides were deparaffinized and rehydrated to distilled water. Antigen retrieval was performed with 1 mM EDTA for 15 minutes at 95°C. Following a normal goat serum block, sections were incubated with the 1:100 diluted primary antibody overnight. Sections were rinsed and incubated with biotinylated goat anti-rabbit IgG, followed by ABC Elite reagent. 3,3' Diaminobenzidine (DAB) was used for detection. Slides were counterstained with hematoxylin and covered with coverslip.

Commercially available tissue array blocks BL2081 and BL 806 (Biomax, Rockville, MD) were similarly stained with anti-EGFR antibody to detect the expression of EGFR in bladder tumors of various stages, grades, and histologies as well as adjacent normal bladder tissues. There were a total of 288 samples with 232 tumors, 8 normal samples, and 48 normal adjacent tumor samples. Of the malignant samples, 86 (36%) were Ta/T1, 108 (47%) were T2, and 38 (16%) were T3. The majority of the malignant samples (197, 85%) were pure urothelial carcinoma, with 7 adenocarcinomas, 10 mucinous adenocarcinomas, and 18 squamous tumors. Each sample was graded by a single pathologist (D.H.) for staining as follows: 0=<10% of cells positive; 1=10–24%; 2=25–49%; 3=50–74%; 4=75–100%. For the purpose of evaluating the expression of EGFR in tissue microarrays, staining was considered negative for grade 0 and positive for grade 1–4.

Statistical Analysis

Data are expressed as mean ± s.e.m. from experimental triplicates. Statistical analysis was carried out by the statistical software, GraphPad Prism. Student’s t test with Mann-Whitney analysis was used to compare the treatment and control effects. Chi squared was performed for categorical variables. $P<0.05$ was used as an indicator of statistically significant difference.

Results

EGFR is Expressed in Bladder Cancer

Of the 232 malignant samples, 69 (30%) had <10% staining (grade 0), and 163 (70%) had grade 1 or higher staining. Of those with positive staining, 43 (19%) had grade 1 staining, 11 (5%) had grade 2 staining, 36 (16%) had grade 3 staining, and 73 (31%) had grade 4 staining (Fig. 1A). There was no relationship between EGFR staining and T stage in our analysis (P=0.9). There was a significantly higher rate of any staining for squamous tumors (17/18, 94%) versus non-squamous tumors (147/214,69%), P=0.04 (Fig. 1B).

EGFR is Expressed in Bladder Cancer Cell Lines

The expression of EGFR on the cell surface of various bladder cancer cell lines was examined using flow cytometry without fixation or permeabilization of the cells. The experiment was carried out at 4°C to limit internalization of EGFR. The breast cancer cell line MDA-MB-453, a HER-2 (ErbB2) positive cell line, was used as a negative control cell line for EGFR (Supplemental Fig. 1A), while, the epidermoid carcinoma cell line, A431, expressing about 2 million EGF-binding EGFRs, was used as a positive control cell line (Supplemental Fig. 1B) (15). The normal urothelial cell line (UPS 54) was used to establish baseline urothelial EGFR expression (Supplemental Fig. 1C). As seen from Fig. 1C, UMUC-5 and ScaBER, the cell lines derived from squamous cell carcinoma (SCC) of the bladder, have very high expression of EGFR (approaching the levels seen in A431 cells) (Supplemental Figs. 1D & 1E). ScaBER and UMUC-5 are basal-like cell lines (16) and consequently highly express EGFR. On the other hand, ‘non-basal-like’ cell lines such as T24, TCCSUP and RT4 (Supplemental Figs. 1F–H) (and metastatic derivatives of T24, T24T, FL3 and SLT3(17)) have comparatively lower expression of cell surface EGFR (Fig. 1C). However, all of the bladder cancer cell lines that we have evaluated, with the exception of RT4, still have significant EGFR expression as compared to the negative control MDA-MB-453 cell line and the normal urothelial cells (UPS 54).

In Vitro Characterization of Pan IR700 Conjugate

Conjugation of panitumumab with IRDye 700Dx NHS ester resulted in approximately three to four IR700 molecules conjugated to each antibody molecule. IR 700 conjugated panitumumab did not show any aggregation based on both Coomassie Brilliant Blue stained gels as well as infrared images of SDS PAGE gels (Supplemental Fig. 2A). The conjugation of IRDye 700Dx to panitumumab could theoretically lead to the loss of EGFR binding but this was ruled out in a flow cytometry experiment of UMUC-5 cells incubated with pan IR700. The median fluorescent intensity of pan IR700 binding is 605 times more than that of cells alone (Supplemental Fig. 2B) indicating no reduction in binding as a consequence of conjugation.

Pan IR700-Based PIT Leads to Rapid Cell Death in EGFR-Expressing Cells

The amount of NIR light needed to induce discernible morphologic changes on light microscopy differed for individual cell lines based on surface EGFR expression. After incubation with pan IR700 (10μg/ml) for one hour, individual 35-mm dishes of UMUC-5,

5637 and UMUC-3 were irradiated with increasing amounts of NIR (0, 4, 20, 32, 64 and 100 J/cm^2). About one hour later, light microscopy images were collected from these plates followed by addition of CellTiter-Glo to detect the viability of cells. Clear morphologic changes were observed in UMUC-5 at 4 J/cm^2 (Supplemental Fig. 3A), in 5637 at 32 J/cm^2 (Supplemental Fig. 3C) and in UMUC-3 at 64 J/cm^2 (Supplemental Fig. 3E). These changes include loss of stellate morphology with cells becoming more round and turgid. There is a concomitant loss of viability in these cells lines at the above mentioned NIR amounts as seen from Supplemental Figs. 3B, 3D and 3F, **respectively**.

The cytotoxic effect of pan IR700-based PIT on UMUC-5 cells was examined using LIVE/DEAD reagent. This reagent specifically stains dead cells that are subsequently analyzed by flow cytometry. After incubation with pan IR700 for one hour, UMUC-5 cells were exposed to 4 J/cm^2 of NIR. Within 30 minutes post-NIR, more than 60% cells of the pan IR700 treated cells were stained with LIVE/DEAD reagent, indicating rapid cell death (Fig. 2A). In a blocking condition to confirm specificity of pan IR700 for EGFR, cells were incubated initially with excess panitumumab and then with pan IR700. Subsequent NIR resulted in only 20% cell death (similar to the cytotoxicity seen with pan alone); thus demonstrating the specificity of pan IR700 based PIT for EGFR. In addition, UMUC-5 cells treated only with 4 J/cm^2 of NIR, pan IR700 with no NIR, and pan with NIR demonstrated little to no cytotoxicity. Similarly, when 5637 cells were treated with the same conditions followed by irradiation with 32 J/cm^2 NIR (Supplemental Fig. 4). Cell death (41%) was only observed in the cells treated with pan IR700 + 32 J/cm^2 of NIR. No cell death was seen in any other conditions. These data demonstrate that both pan IR700 and its excitation by NIR are required for cell death. Panitumumab, even when incubated with cells for 96 hours, demonstrated little to no effect on the survival of the bladder cancer lines tested (UMUC-5, TCCSUP, 5637 and RT4) (Supplemental Fig. 5A). Similarly, IR700 dye alone did not induce phototoxicity in UMUC-5 cells, except at a very high concentration of 1 μM and at a very high NIR dose of 100 J/cm^2 (Supplemental Fig. 5B). Our preliminary work reveals that most experiments require a dose of 10 μg/mL of pan IR700, which generally contains ~100 nM of IR 700Dx, associated with the monoclonal antibody. This dose of dye demonstrated no overt toxicity at either 4 J/cm^2 or 100 J/cm^2.

Potency of Pan IR700-Based PIT Depends Upon the Amount of EGFR Expression in Cells

The IC$_{50}$ of pan IR700 NIR-PIT for UMUC-5 cells was calculated by incubating the cells with increasing concentrations of pan IR700 followed by irradiation with 4 J/cm^2 of NIR. The IC$_{50}$ for UMUC-5 cells under these conditions was 4.7 nM for pan IR700 (Fig. 2B(i)). Other bladder cancer cell lines expressing less EGFR compared to UMUC-5, such as TCCSUP, 5637 and T24, did not show any cell death at 4 J/cm^2 of NIR. The minimum amount of NIR required for demonstrating pan IR700 based phototoxicity was 64 J/cm^2 for TCCSUP, T24 and UMUC-3 and 32 J/cm^2 for 5637 (Supplemental Fig. 3). The IC$_{50}$ of pan IR700 for 5637 at 32 J/cm^2 is 5.8 nM, TCCSUP cells at 64 J/cm^2 is 4 nM, and for UMUC-3 at 64 J/cm^2 is 108 nM (Fig. 2B (ii, iii & iv, **respectively)**) indicating there is an inverse relation between the surface expression of EGFR and the amount of NIR required to achieve the nanomolar range IC$_{50}$s (Fig. 2C). As a control, normal urothelial cells, UPS54 were

treated with 10 μg/ml of pan IR700 and 100 J/cm^2 of NIR. These cells do not show any cell death 6 hours post-NIR (Supplemental Fig. 6).

Pan IR700-based PIT Induces Necrotic Cell Death

UMUC-5 cells treated with pan IR700 were irradiated with NIR of 4 J/cm^2. Twenty minutes post NIR, a single cell suspension of these cells was treated with FITC annexin V and FxCycle Violet and then analyzed by flow cytometry. UMUC-5 cells treated with the apoptosis inducer, staurosporine (1μM), for 3 hours were used as a positive control for adjusting the voltages for FSC, SSC, FITC and Pacific Blue filters (Supplemental Fig. 7). As seen from Fig. 3A, about 50% of the pan IR700-treated cells localize to the upper right quadrant (high annexin V/ high FxCycle Violet staining), representing cells in the late apoptosis/early necrosis stage of cell death. Only 35% of cells remained in the lower left quadrant which are live cells with low Annexin V and low FxCycle violet. No treatment, pan IR700 without NIR, and panitumumab or IR700 dye with or without NIR result in some inadvertent cell death due to the use of trypsin for preparation of single cell suspension. Unfortunately, other methods of single cell preparation such as accutase or EDTA are too mild for these cells to prepare single cell suspension whereas cell scraping resulted in far more incidental cell death. However, most of the cells treated with these conditions remain in the lower left (low annexin V FITC/low FxCycle) quadrant. This again confirms the previous experiments demonstrating cell death only in the condition of pan IR700 activated by NIR. Of note, cell death in PIT is rapid as annexin V/FxCycle staining at 60 minutes reveals very few events on forward scatter and side scatter plots of flow cytometry due to rapid cell death (Supplemental Fig. 8). Such rapid cell death suggests necrosis.

In order to rule out the induction of apoptosis as the primary mechanism of cell death in PIT-treated cells, the Caspase-Glo 3/7 assay was performed with UMUC-5, 5637, and UMUC-3 cells. This assay detects cleaved caspase 3 and 7 and is a direct measure of the end-products of apoptosis. As seen from Fig. 3B (ii), none of the cells treated with pan IR700 and cytotoxic NIR doses demonstrated any caspase 3/7 activation over and above untreated controls or non-NIR treated controls (Fig. 3B (i)). The known apoptosis inducer staurosporine (1μM) was used as a positive control. This treatment resulted in the production of significantly elevated levels of cleaved caspase 3/7 which were inhibited by the cell permeable caspase-specific inhibitor Z-VAD-FMK. The addition of Z-VAD-FMK did not alter the levels of cleaved caspase 3/7 in PIT treated (pan IR700 + NIR) cells.

In order to establish necrotic cell death definitively, transmission electron microscopy (TEM) was performed. TEM is considered the “gold standard” for determining the mechanism of cell death (18). As seen in Fig. 3C, the pan IR700-based PIT-treated cells on the right (Fig. 3C(ii)) are considerably larger compared to normal cells (Fig. 3C(i)). The plasma membrane is mostly disintegrated in these cells. The integrity of the nuclear membrane is compromised; nucleoplasm and cytoplasm appear to be depleted of all material. Although some mitochondria are surprisingly normal, most other organelles appear to be swollen. These are the classic findings of late necrotic cells, thus confirming that pan IR700-NIR-PIT causes necrotic cell death.

Reactive and Singlet Oxygen Species are generated in NIR-PIT

Reactive oxygen species (ROS) were measured using a cell permeable reagent called 2',7'-dichlorofluorescein diacetate (DCFDA). DCFDA is a fluorogenic dye that gets oxidized to 2',7'-dichlorofluorescin, a highly fluorescent moiety detected by fluorescent spectroscopy, in the presence of ROS. As seen from Fig. 4A, both pan IR700 and IR700 dye-treated UMUC-5 cells previously incubated with DCFDA demonstrate a three- to four-fold increase in fluorescence just 5 minutes post NIR activation, suggesting the production of a large excess of ROS. Trolox, a water soluble, ROS-specific scavenger, was able to inhibit this ROS generation. Moreover, ROS were specifically generated only when IR700 was present and NIR was delivered. As a result, pan IR700 and IR700 treated cells in the absence of NIR displayed baseline levels of ROS production similar to untreated or panitumumab treated UMUC-5 cells with or without NIR (Supplemental Fig. 9A & 9B).

Singlet oxygen species (SOS) were measured using Singlet Oxygen Sensor Green (SOSG) reagent. In the presence of SOS, this reagent emits green fluorescence similar to fluorescin. As shown in Fig. 4B, UMUC-5 cells pre-incubated with SOSG, and treated with either pan IR700 or IR700 produce four-fold more SOS in the presence of NIR compared to baseline levels (non-NIR conditions or untreated or panitumumab only treated cells). Again, this SOS production happens rapidly in the first 5 minutes post NIR treatment and can be quenched to baseline levels in the presence of the SOS-specific scavenger, sodium azide (NaN_3).

When cell survival assay was carried out in the presence of trolox and sodium azide (specific scavengers of ROS and SOS, respectively), only sodium azide was able to rescue UMUC-5 cells from pan IR700-based PIT. Therefore, although both ROS and SOS are produced during pan IR700-based PIT, SOS likely contributes more significantly toward cell death than ROS. Furthermore, although IR700 dye alone produces both ROS and SOS, the production in the absence of targeting the cell membrane of EGFR expressing cancer cells does not cause any cell death (Fig. 4C).

Pan IR700-based PIT Reduces Tumor Burden in Bladder Cancer Xenografts

About 3 million UMUC-5 cells resuspended in 50% Matrigel in 1× PBS were injected subcutaneously in the right thigh of female athymic Nu/Nu mice to generate UMUC-5 xenografts. Seven days post injection, xenograft tumors of size ~ 50–100 mm^3 were observed. The H & E staining of these tumors indicated squamous morphology retained in UMUC-5 tumors (Fig. 5A(i)). Moreover, staining of hEGFR indicated UMUC-5 tumors maintained high hEGFR expression in xenografts similar to cells *in vitro* (Fig. 5A(ii)). To elucidate the effect of pan IR700 on xenografts, athymic nude mice bearing UMUC-5 tumors were injected with 120 μg of pan IR700. One group of mice (n=10) was treated with 100 J/cm^2 and 50 J/cm^2 of NIR 24 and 48 hours post-pan IR700 treatment, respectively. The NIR treatment was given focally in the area of subcutaneous tumor by placing the light source just above the tumor. The other group of mice (n=10) was not treated with any NIR. As seen from Fig. 5B, the growth of NIR treated tumors is attenuated in comparison to non-NIR treated tumors. In fact, three of ten NIR treated tumors regressed completely and therefore could not be measured by external calipers during the period of experiment (Supplemental Fig. 10B). On the other hand, non-NIR treated tumors did not slow down

their growth as seen in Supplemental Fig 10A, where tumor volumes of individual mice are plotted as a function of time. The tumor weights measured at the end of the experiment showed that non-NIR treated tumors were significantly larger (median weight – 0.5g) than NIR treated tumors (median weight – 0.2g) (two tailed P-test, Mann-Whitney Analysis, P=0.0077 (Fig. 5C)). On the other hand, when the same experiment was repeated with UMUC-3, a cell line with considerably lower EGFR surface expression, there was no difference in the growth of tumors irradiated or non-irradiated with NIR (Supplemental Fig. 11). This data highlights both the importance of expression of the targeted cell surface antigen as well as the specificity of this treatment.

Discussion

We demonstrate a novel therapy in bladder cancer cell lines called molecular targeted photoimmunotherapy (PIT) (14). In this method, a humanized monoclonal antibody against a specific target is conjugated to a photoabsorbing dye and this conjugate is then activated by NIR after sufficient time to allow cell binding. IR700 functions as a photo-absorber instead of a traditional photosensitizer because, in its non-conjugated state, it does not result in generalized cytotoxicity when activated by NIR. In our study, EGFR was chosen as the target given its high rate of amplification in bladder cancer. However, this therapy does not require addiction to the EGFR pathway; instead, it merely requires relatively high surface expression of EGFR in tumor cells as compared to normal cells. The lack of addiction to the EGFR pathway (due to downstream mutations and alternate signaling pathways) and the inability to reproduce ADCC in the absence of an immune system are likely reasons for the relative inefficacy of panitumumab alone in our studies(19–21). We demonstrate successful conjugation of IR700 to panitumumab and the resulting conjugate induces cell death in EGFR-expressing cell lines at low doses of NIR. For instance, these light doses do not produce significant thermal effects on the treated surface. Furthermore, cell death only occurs in cells that express EGFR on their surfaces and only in the presence of NIR and the pan IR700 conjugate.

We also demonstrated that cell death occurs by necrosis. First, rapid cell death within 60 minutes of NIR suggests necrosis. Second, the FITC annexin V – FxCycle violet assay demonstrates localization of treated cells to the late apoptosis/early necrosis quadrant at 20 minutes. At 20 minutes, this is more consistent with early necrosis. At the same time there was no generation of cleaved caspase 3/7. Finally, transmission electron microscopy shows preservation of mitochondria but considerable disruption of the plasma membrane. Most lipophilic photosensitizers associated with PDT (e.g. Photofrin) localize to the mitochondria and induce apoptosis through mitochondrial disruption, release of cytochrome c, and activation of the intrinsic pathway of apoptosis (22). Because of their lipophilicity they tend to enter both normal and neoplastic cells leading to collateral damage. Conversely, photosensitizers localized to the plasma membrane are likely to cause necrosis. The IR700 dye is hydrophilic and therefore does not freely enter cells. However, the antibody-conjugated IR700 binds to specific cell surface receptors and when exposed to NIR, rapid cell damage ensues. The exact mechanism of action of PIT is still uncertain. We demonstrate that NIR-PIT produces ROS and SOS suggesting that oxidative damage may cause degradation of membrane lipids leading to rupture and necrosis, although we did not detect

any oxidative changes on major unsaturated lipid molecules after NIR-PIT so far. IR700 by itself produces a large amount of SOS but does not cause cell death likely because the molecule is sufficiently far away from the cell membrane and SOS have an extremely transient lifespan of <0.04 microseconds in biologic systems and a very narrow radius of activity at <0.02 micrometers (23). However, pan IR700 bound to EGFR and activated by NIR releases SOS at the plasma membrane to induce localized necrosis. Finally, singlet oxygen also has a direct cytotoxic effect on local tumor cells and vasculature and can attract dendritic cells and neutrophils thereby initiating an acute inflammatory response (24). Free radical scavengers reduced the effect of NIR-PIT, although this has not been universally true (25,26).

The bladder is a well-suited organ for light therapy given the easy accessibility via cystoscopy and the need to treat the entire organ due to the multifocal nature of bladder cancer. Kelly *et al* first demonstrated photodynamic destruction of bladder cancers implanted in mice using a hematoporphyrin derivative (HPD) in 1975 (27). Subsequently, they conducted the first human clinical trial showing preferential localization of HPD in malignant and pre-malignant urothelium with tumor destruction upon illumination of these areas (28). However, HPD fluorescence was also present in normal urothelium. There is no difference in light penetration between benign and malignant bladder tissue; therefore, toxicity from therapy was a major limitation (29). In addition, HPD was given intravenously which can result in systemic accumulation and cutaneous phototoxicity for many weeks. Despite the introduction of newer PS such as 5-aminolevulinic acid (5-ALA), Photofrin I, Photofrin II, and hexaminolevulinate (HAL), toxicities such as irritative urinary symptoms, skin photosensitivity, and bladder contracture still occurred in clinical trials. Furthermore, late responses to PDT in these trials were quite variable ranging from 11–64% (30). Although an initial report with a novel PS called Radachlorin is promising with a recurrence-free rate of 64.4% at 2 years with minimal toxicity (30), a previous report with a similar chlorine containing compound reported a case of vesicoenteric fistula as a complication (31). Therefore, most prior phototherapies have failed due to their side effects.

Epidermal growth factor receptor (EGFR) has been previously targeted using the EGFR humanized chimeric monoclonal antibody C225 (cetuximab) conjugated to a benzoporphyrin derivative (verteporfin) successfully in cancer cell lines (32). However, the biodistribution of this conjugate has made it difficult to treat bladder cancers selectively while avoiding generalized phototoxicity. In our current study, we also used an anti-EGFR humanized monoclonal antibody, panitumumab, but applied it to bladder cancer cell lines. What is different about the current work is the use of a phthalocyanine dye called IR700 instead of a porphyrin derivative. Unlike 5-ALA or the hematoporphyrin derivatives, IR700 is completely water soluble hence, free, unconjugated dye gets rapidly excreted in urine without accumulation within the body resulting in no photosensitizing effect (Supplement Fig. 5B and C; and (14)). Compared to conventional photosensitizers, it has a greater than fivefold higher extraction coefficient that allows rapid elimination from the blood/plasma (14). Furthermore, it is not toxic to normal tissues or phototoxic upon NIR and so it is theoretically safer than traditional photosensitizers. The pan IR700 conjugate differs from PDT in that internalization of the conjugate is not required in order to induce cell death. Finally, since IR700 uses a higher wavelength of light, it can penetrate tissue more deeply

than the wavelengths of light needed to activate traditional PS. For example, light at 693 nm penetrates 40% deeper than light at 633 nm ($P<0.002$) (29). NIR at 693 nm has a potential depth of penetration of 1–2 cm. Since the average bladder wall thickness is 3.35 mm, we believe that this may be a viable therapy for bladder cancer in the future (33).

In this pre-clinical manuscript, we evaluated the effect of PIT in subcutaneous xenografts. Although the intravesical approach is ideal for future use in bladder cancer therapy, pre-clinical intravesical therapy is not as straight forward. Although we attempted direct inoculation of UMUC-5 and other cell lines intravesically in nude mice to establish orthotopic intravesical human tumors, the tumor formation rate was <10% and in animals where tumor developed, it spontaneously regressed in certain cases. Therefore, we did not feel this was a reliable model to pursue and hence the work in this paper focuses on subcutaneous tumors. The best published approaches of inducing orthotopic tumors involve either a carcinogen model or implantation of isogenic MB49 cells in C57/BL6 mice (34). However, both of these approaches may lead to mouse-EGFR (mEGFR) bearing tumors and we cannot test the panitumumab-IR700 conjugate in such models because panitumumab does not cross-react with mEGFR (35). In the future, we will embark on orthotopic models to directly evaluate intravesical therapy with PIT but this initial work used subcutaneous xenografts to prove that human tumors can be treated.

The prevalence of EGFR expression in bladder cancer cell lines makes it a viable therapy in at least basal-like tumors. Molecular stratification reveals that the basal phenotype, which is enriched for EGFR activation/amplification, can be found in almost 25% of bladder tumors (16). Furthermore, squamous differentiation is extremely common in UCC and increases with T stage and can be as high as 60–80% in T3 tumors (36). Although SCC of the bladder is often locally advanced, it does not metastasize as often as urothelial cancer, potentially allowing for localized therapy as well (12). Perhaps our strategy may be applicable to any bladder tumor with a basal phenotype and now this can be assessed using BASE47, a gene set predictor, that can distinguish between basal and luminal molecular subtypes of bladder cancer (37). Moreover, this strategy can be extended to other cell surface proteins over-expressed or aberrantly expressed on bladder cancer cells, such as FGFR-3, ErbB-2, Nectin-4, Muc-1 and CEA to name a few. UMUC-3, a low EGFR-expressing cell line, did not respond well to pan IR700-mediated PIT both in vitro and in xenografts. In order to treat such a cell line or cancer, the use of other cell surface antigens or a cocktail of several different monoclonal antibodies conjugated to a PA like IR700 will need to be employed. This is the goal of a future project. However, other targets and combinations are available. For example, a urothelial cancer cell line with the lowest level of EGFR surface expression, RT4, actually has the highest ErbB-2 expression and our preliminary data demonstrate that it may be amenable to an anti-ErbB-2-IR700 approach (M.R. Siddiqui; unpublished observations).

In summary, we describe a proof-of-concept study of molecular targeted PIT in bladder cancer cells using a panitumumab IR700 conjugate. Given the high amplification rate of EGFR in most bladder cancers, it may provide a selective and novel therapy for non-muscle invasive bladder cancer. We are actively conducting orthotopic murine models with this

therapy and hope that our efforts translate into a clinically viable strategy for bladder cancer patients in the future.

Supplementary Material

Refer to Web version on PubMed Central for supplementary material.

Acknowledgments

This research was supported by the Intramural Research Program of the NIH, National Cancer Institute, Center for Cancer Research. We thank Ms. Catherine Wells for maintenance of animal facility and technical support with animal work. Special thanks to Ms. Donna Butcher from Pathology/Histotechnology Laboratory, NCI for staining of TMAs. We thank Dr. Ulrich Baxa from Electron Microscopy Core Facility of NCI for help with TEM.

Financial Information – P.K. Agarwal - NIH intramural grant number ZIABC011458-02

References

1. Siegel RL, Miller KD, Jemal A. Cancer statistics, 2016. CA Cancer J Clin. 2016; 66(1):7–30. DOI: 10.3322/caac.21332 [PubMed: 26742998]
2. Botteman MF, Pashos CL, Redaelli A, Laskin B, Hauser R. The health economics of bladder cancer: a comprehensive review of the published literature. PharmacoEconomics. 2003; 21(18):1315–30. [PubMed: 14750899]
3. O'Donnell MA, Boehle A. Treatment options for BCG failures. World journal of urology. 2006; 24(5):481–7. DOI: 10.1007/s00345-006-0112-0 [PubMed: 17021823]
4. Stein JP, Lieskovsky G, Cote R, Groshen S, Feng AC, Boyd S, et al. Radical cystectomy in the treatment of invasive bladder cancer: long-term results in 1,054 patients. Journal of clinical oncology : official journal of the American Society of Clinical Oncology. 2001; 19(3):666–75. [PubMed: 11157016]
5. Chaux A, Cohen JS, Schultz L, Albadine R, Jadallah S, Murphy KM, et al. High epidermal growth factor receptor immunohistochemical expression in urothelial carcinoma of the bladder is not associated with EGFR mutations in exons 19 and 21: a study using formalin-fixed, paraffin-embedded archival tissues. Human pathology. 2012; 43(10):1590–5. DOI: 10.1016/j.humpath.2011.11.016 [PubMed: 22406363]
6. Rotterud R, Nesland JM, Berner A, Fossa SD. Expression of the epidermal growth factor receptor family in normal and malignant urothelium. BJU international. 2005; 95(9):1344–50. DOI: 10.1111/j.1464-410X.2005.05497.x [PubMed: 15892828]
7. Comprehensive molecular characterization of urothelial bladder carcinoma. Nature. 2014; 507(7492):315–22. DOI: 10.1038/nature12965 [PubMed: 24476821]
8. Messing EM. Clinical implications of the expression of epidermal growth factor receptors in human transitional cell carcinoma. Cancer research. 1990; 50(8):2530–7. [PubMed: 1690599]
9. Abol-Enein H, Kava BR, Carmack AJK. Nonurothelial Cancer of the Bladder. Urology. 2007; 69(1, Supplement):93–104. doi http://dx.doi.org/10.1016/j.urology.2006.08.1107. [PubMed: 17280911]
10. Martin JE, Jenkins BJ, Zuk RJ, Blandy JP, Baithun SI. Clinical importance of squamous metaplasia in invasive transitional cell carcinoma of the bladder. J Clin Pathol. 1989; 42(3):250–3. [PubMed: 2703540]
11. Hayashi T, Sentani K, Oue N, Anami K, Sakamoto N, Ohara S, et al. Desmocollin 2 is a new immunohistochemical marker indicative of squamous differentiation in urothelial carcinoma. Histopathology. 2011; 59(4):710–21. DOI: 10.1111/j.1365-2559.2011.03988.x [PubMed: 22014052]
12. Guo CC, Gomez E, Tamboli P, Bondaruk JE, Kamat A, Bassett R, et al. Squamous cell carcinoma of the urinary bladder: a clinicopathologic and immunohistochemical study of 16 cases. Human pathology. 2009; 40(10):1448–52. DOI: 10.1016/j.humpath.2009.03.005 [PubMed: 19454359]

13. Guo CC, Fine SW, Epstein JI. Noninvasive squamous lesions in the urinary bladder: a clinicopathologic analysis of 29 cases. The American journal of surgical pathology. 2006; 30(7): 883–91. DOI: 10.1097/01.pas.0000213283.20166.5a [PubMed: 16819332]

14. Mitsunaga M, Ogawa M, Kosaka N, Rosenblum LT, Choyke PL, Kobayashi H. Cancer cell-selective in vivo near infrared photoimmunotherapy targeting specific membrane molecules. Nature medicine. 2011; 17(12):1685–91. DOI: 10.1038/nm.2554

15. Fernandez-Pol JA. Epidermal growth factor receptor of A431 cells. Characterization of a monoclonal anti-receptor antibody noncompetitive agonist of epidermal growth factor action. The Journal of biological chemistry. 1985; 260(8):5003–11. [PubMed: 2985573]

16. Rebouissou S, Bernard-Pierrot I, de Reynies A, Lepage ML, Krucker C, Chapeaublanc E, et al. EGFR as a potential therapeutic target for a subset of muscle-invasive bladder cancers presenting a basal-like phenotype. Science translational medicine. 2014; 6(244):244ra91.doi: 10.1126/scitranslmed.3008970

17. Nicholson BE, Frierson HF, Conaway MR, Seraj JM, Harding MA, Hampton GM, et al. Profiling the evolution of human metastatic bladder cancer. Cancer research. 2004; 64(21):7813–21. DOI: 10.1158/0008-5472.CAN-04-0826 [PubMed: 15520187]

18. Krysko DV, Vanden Berghe T, D'Herde K, Vandenabeele P. Apoptosis and necrosis: detection, discrimination and phagocytosis. Methods. 2008; 44(3):205–21. DOI: 10.1016/j.ymeth.2007.12.001 [PubMed: 18314051]

19. Earl J, Rico D, Carrillo-de-Santa-Pau E, Rodriguez-Santiago B, Mendez-Pertuz M, Auer H, et al. The UBC-40 Urothelial Bladder Cancer cell line index: a genomic resource for functional studies. BMC Genomics. 2015; 16:403.doi: 10.1186/s12864-015-1450-3 [PubMed: 25997541]

20. Schneider-Merck T, Lammerts van Bueren JJ, Berger S, Rossen K, van Berkel PH, Derer S, et al. Human IgG2 antibodies against epidermal growth factor receptor effectively trigger antibody-dependent cellular cytotoxicity but, in contrast to IgG1, only by cells of myeloid lineage. Journal of immunology. 2010; 184(1):512–20. DOI: 10.4049/jimmunol.0900847

21. Monteverde M, Milano G, Strola G, Maffi M, Lattanzio L, Vivenza D, et al. The relevance of ADCC for EGFR targeting: A review of the literature and a clinically-applicable method of assessment in patients. Crit Rev Oncol Hematol. 2015; 95(2):179–90. DOI: 10.1016/j.critrevonc.2015.02.014 [PubMed: 25819749]

22. Dougherty TJ, Gomer CJ, Henderson BW, Jori G, Kessel D, Korbelik M, et al. Photodynamic therapy. Journal of the National Cancer Institute. 1998; 90(12):889–905. [PubMed: 9637138]

23. Moan J, Berg K. The photodegradation of porphyrins in cells can be used to estimate the lifetime of singlet oxygen. Photochemistry and photobiology. 1991; 53(4):549–53. [PubMed: 1830395]

24. Moore CM, Pendse D, Emberton M. Photodynamic therapy for prostate cancer--a review of current status and future promise. Nature clinical practice Urology. 2009; 6(1):18–30. DOI: 10.1038/ncpuro1274

25. Jin J, Krishnamachary B, Mironchik Y, Kobayashi H, Bhujwalla ZM. Phototheranostics of CD44-positive cell populations in triple negative breast cancer. Sci Rep. 2016; 6:27871.doi: 10.1038/srep27871 [PubMed: 27302409]

26. Shirasu N, Yamada H, Shibaguchi H, Kuroki M, Kuroki M. Potent and specific antitumor effect of CEA-targeted photoimmunotherapy. International journal of cancer Journal international du cancer. 2014; 135(11):2697–710. DOI: 10.1002/ijc.28907 [PubMed: 24740257]

27. Kelly JF, Snell ME, Berenbaum MC. Photodynamic destruction of human bladder carcinoma. British journal of cancer. 1975; 31(2):237–44. [PubMed: 1164470]

28. Kelly JF, Snell ME. Hematoporphyrin derivative: a possible aid in the diagnosis and therapy of carcinoma of the bladder. The Journal of urology. 1976; 115(2):150–1. [PubMed: 1249866]

29. Shackley DC, Whitehurst C, Moore JV, George NJ, Betts CD, Clarke NW. Light penetration in bladder tissue: implications for the intravesical photodynamic therapy of bladder tumours. BJU international. 2000; 86(6):638–43. [PubMed: 11069369]

30. Lee JY, Diaz RR, Cho KS, Lim MS, Chung JS, Kim WT, et al. Efficacy and safety of photodynamic therapy for recurrent, high grade nonmuscle invasive bladder cancer refractory or intolerant to bacille Calmette-Guerin immunotherapy. The Journal of urology. 2013; 190(4):1192–9. DOI: 10.1016/j.juro.2013.04.077 [PubMed: 23648222]

31. Lee LS, Thong PS, Olivo M, Chin WW, Ramaswamy B, Kho KW, et al. Chlorin e6-polyvinylpyrrolidone mediated photodynamic therapy--A potential bladder sparing option for high risk non-muscle invasive bladder cancer. Photodiagnosis and photodynamic therapy. 2010; 7(4): 213–20. DOI: 10.1016/j.pdpdt.2010.08.005 [PubMed: 21112542]

32. Savellano MD, Hasan T. Photochemical targeting of epidermal growth factor receptor: a mechanistic study. Clinical cancer research : an official journal of the American Association for Cancer Research. 2005; 11(4):1658–68. DOI: 10.1158/1078-0432.CCR-04-1902 [PubMed: 15746071]

33. Hakenberg OW, Linne C, Manseck A, Wirth MP. Bladder wall thickness in normal adults and men with mild lower urinary tract symptoms and benign prostatic enlargement. Neurourol Urodyn. 2000; 19(5):585–93. [PubMed: 11002301]

34. Gabriel U, Bolenz C, Michel MS. Experimental models for therapeutic studies of transitional cell carcinoma. Anticancer Res. 2007; 27(5A):3163–71. [PubMed: 17970057]

35. Yang XD, Jia XC, Corvalan JR, Wang P, Davis CG, Jakobovits A. Eradication of established tumors by a fully human monoclonal antibody to the epidermal growth factor receptor without concomitant chemotherapy. Cancer research. 1999; 59(6):1236–43. [PubMed: 10096554]

36. Lopez-Beltran A, Requena MJ, Cheng L, Montironi R. Pathological variants of invasive bladder cancer according to their suggested clinical significance. BJU international. 2008; 101(3):275–81. DOI: 10.1111/j.1464-410X.2007.07271.x [PubMed: 17986288]

37. Damrauer JS, Hoadley KA, Chism DD, Fan C, Tiganelli CJ, Wobker SE, et al. Intrinsic subtypes of high-grade bladder cancer reflect the hallmarks of breast cancer biology. Proceedings of the National Academy of Sciences of the United States of America. 2014; 111(8):3110–5. DOI: 10.1073/pnas.1318376111 [PubMed: 24520177]

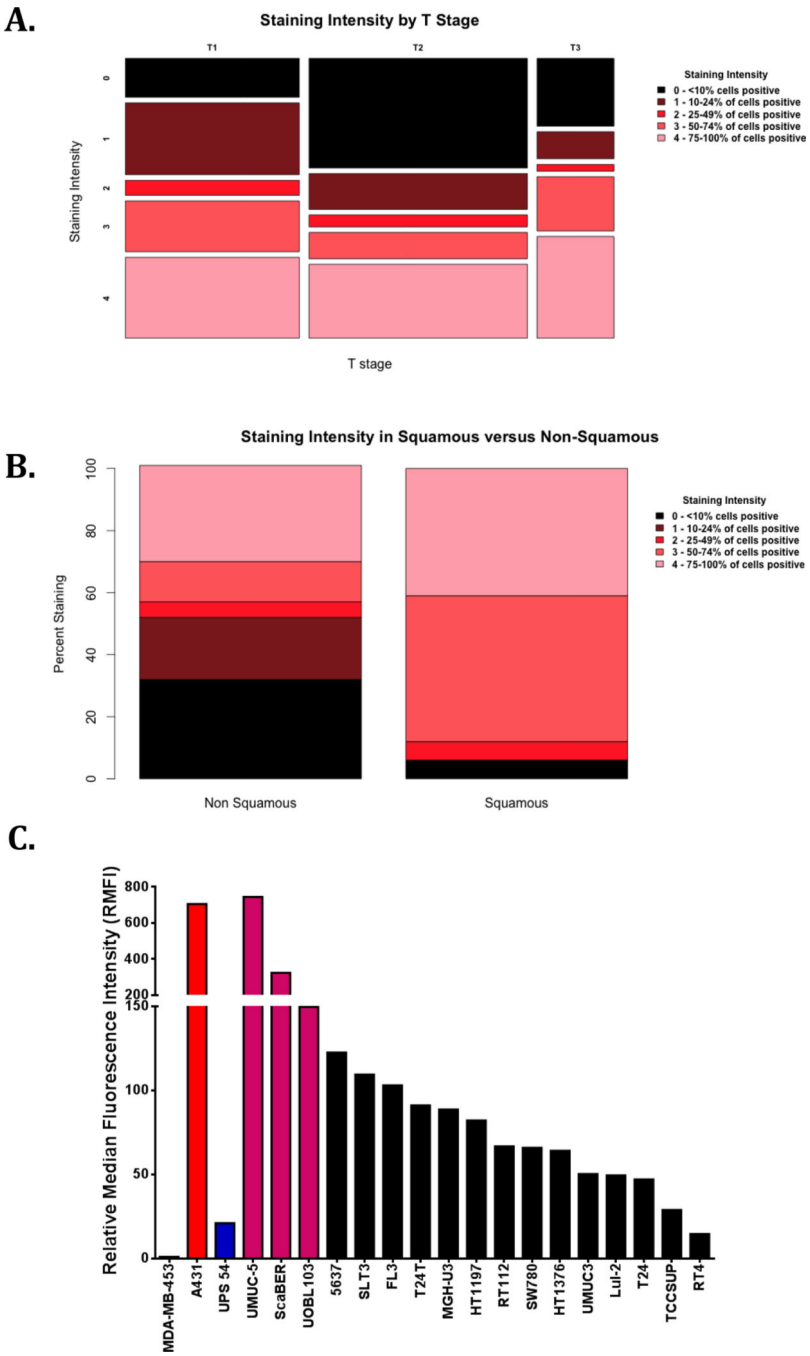

Figure 1. Expression of EGFR in bladder cancer tissues and cell lines

A. Staining intensity of bladder cancer tissue cores by T stage. Tissue microarrays BL2081 and BL806 (Biomax) were analyzed for presence of EGFR expression using anti-EGFR antibody (CST No. 4267). Each sample was graded for staining as follows: 0=<10% of cells positive (black); 1=10–24% (maroon); 2=25–49 % (red); 3=50–74% (firebrick); 4=75–100% (pink). There is no relationship between EGFR staining and T stage.

B. Staining intensity of non-squamous versus squamous bladder cancers. About 94% of bladder SCC cores in our analysis showed very high expression of EGFR (staining intensities 3 and 4) as compared to non-squamous bladder cancer cores.

C. Surface expression of EGFR on various cell lines. Surface expression of EGFR was studied using flow cytometry. Single cell suspension of cell lines was incubated with PE-tagged rat mAB to human EGFR or PE tagged rat IgG2a, kappa mAB (isotype control). The experiment was carried out at 4°C. At the end of 30 minutes of incubation, the cells were washed and analyzed on the flow cytometer. The relative median fluorescence intensity (RMFI) for each cell line was calculated by the following formula:

$$\mathrm{RMFI}=\frac{\mathrm{Median\ \ Fluorescence\ \ Intensity\ (Anti-EGFR)}}{\mathrm{Median\ \ Fluorescence\ \ Intensity\ (Isotype\ \ Control)}}$$

RMFI of various cell lines including the “Gold Standard” for EGFR expression (A431 (red bar)), a normal urothelial cell line (UPS54 (blue bar)), and bladder SCC lines (UMUC5, ScaBER, UOBL103 (pink bar)) are represented in the figure. RMFIs of all urothelial cancer cell lines tested are represented in solid black bars.

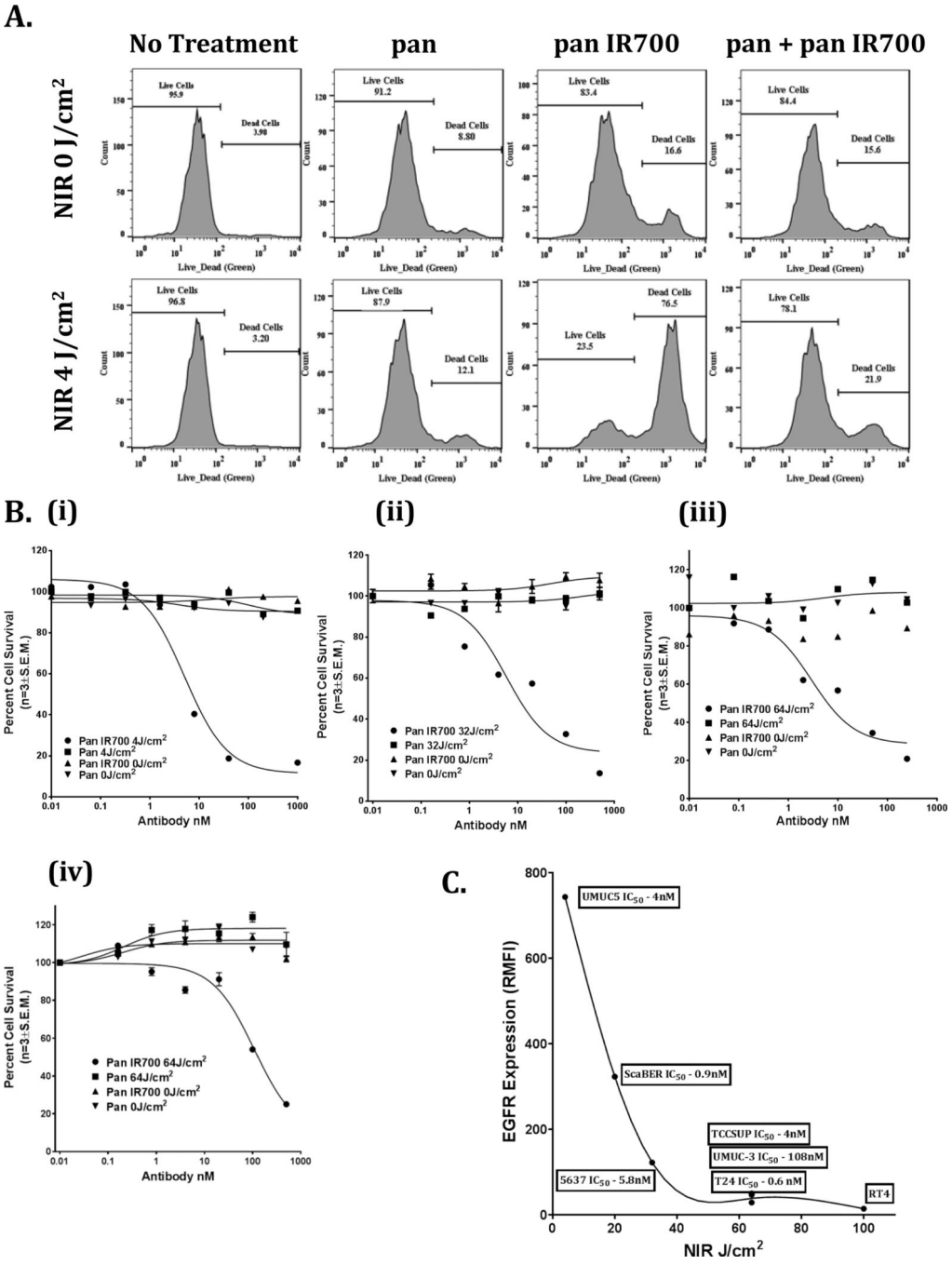

Figure 2. *In Vitro* effects of pan IR700 based PIT on EGFR expressing cells

A. Pan IR700 based PIT induces cell death in UMUC5 cells. Untreated UMUC5 cells, UMUC5 cells treated with panitumumab (10μg/ml), pan IR700 (10μg/ml) and UMUC5 cells pre-treated with panitumumab (50μg/ml) followed by pan IR700 (10μg/ml) were subjected to no NIR (NIR 0 J/cm^2 (upper panel)) or 4 J/cm^2 of NIR (lower panel). Thirty minutes post-NIR treatment, the cell death was measured on flow cytometry using green LIVE/ DEAD reagent (Ex. 488nm/ Em. 535nm). The cell death is observed only in the cells treated with pan IR700 + 4 J/cm^2 NIR. No appreciable cell death was observed under blocking

conditions indicating the specificity of pan IR700 (lower, rightmost panel) for EGFR binding.

B. IC_{50} measurement of pan IR700 mediated PIT for bladder cancer cell lines. UMUC5 (i), 5637 (ii) and TCCSUP (iii) and UMUC-3 (iV) were treated with increasing concentrations of pan IR700 (▲), panitumumab (▼) without NIR treatment or with pan IR700 (●) and panitumumab (■) in the presence of 4 J/cm^2 (UMUC5), 32 J/cm^2 (5637) and 64 J/cm^2 (TCCSUP, UMUC-3) of NIR. After 24 hours, cell survival was monitored using MTS reagent. The data is represented as percent cell survival. The IC50 values for UMUC5, 5637, TCCSUP and UMUC-3 are 4.7nM, 5.8nM, 4 nM and 108nM respectively. No cell death was observed under any other conditions.

C. The amount of NIR required to achieve equivalent amount of cell death (in terms of IC50 values) in bladder cancer cell lines is plotted as a function of cell surface EGFR expression (RMFI). As the expression of EGFR increases, the NIR needed to achieve similar IC_{50} values of pan IR700 decreases.

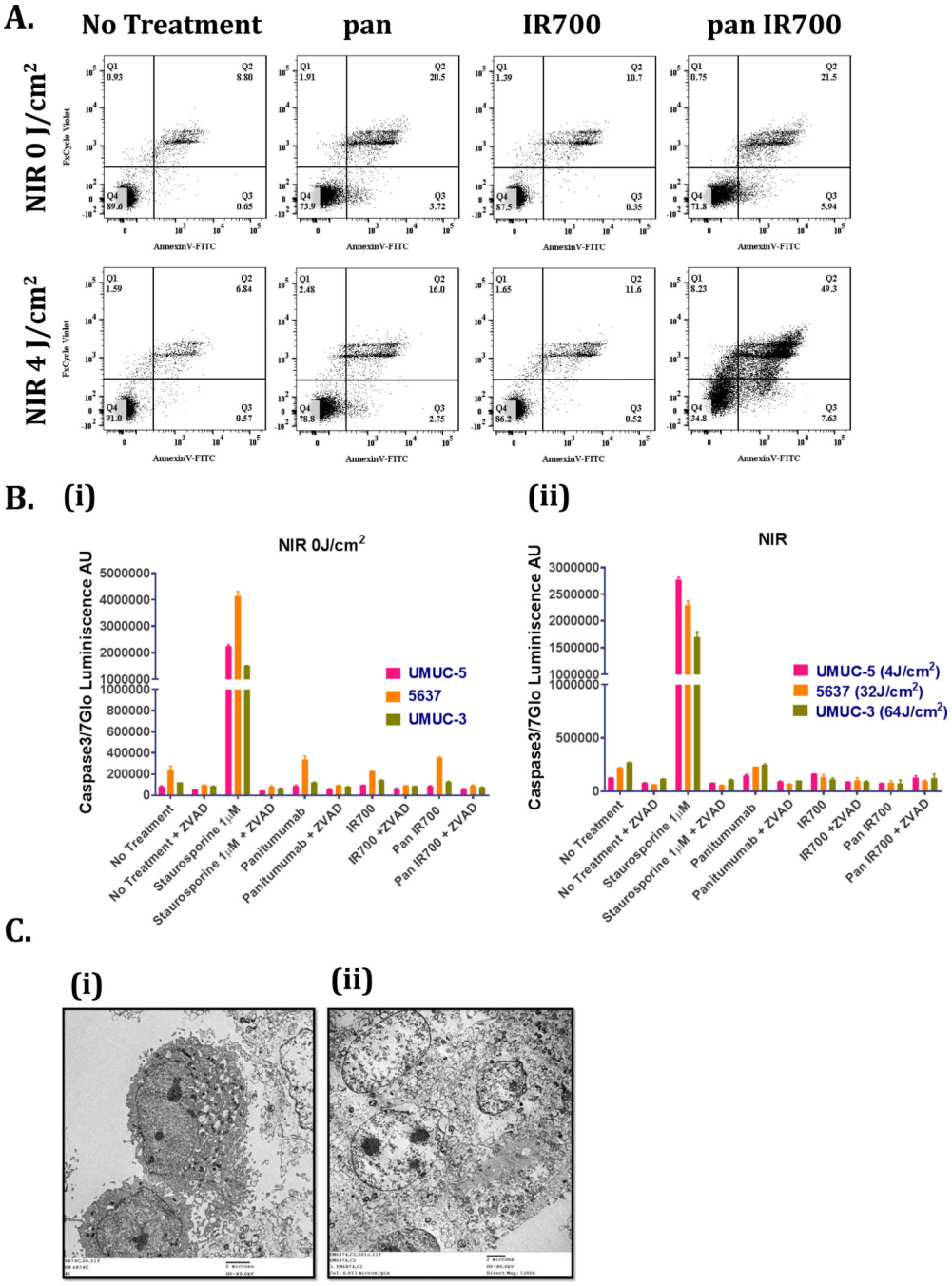

Figure 3. Pan IR700 based PIT induces necrosis

A. Annexin V FITC – FxCycle violet staining indicates necrosis as a mode of cell death in cells treated with pan IR700 mediated PIT. Untreated UMUC-5 cells, UMUC-5 cells treated with panitumumab (10μg/ml), pan IR700 (10μg/ml) and IR700 were subjected to no NIR (NIR 0 J/cm^2 (upper panel)) or 4 J/cm^2 of NIR (lower panel). Twenty minutes post-NIR treatment, the cells were analyzed on flow cytometry by staining cells with Annexin V FITC and FxCycle violet. UMUC5 cells treated with pan IR700 and 4 J/cm^2 of NIR (lower,

rightmost panel) localized mostly to the upper right quadrant (50% cells in late apoptosis/necrosis quadrant) and only 35% cells in the low Annexin V-low FxCycle violet quadrant. **B.** Caspase-Glo 3/7 assay to rule out apoptosis in PIT treated cells. UMUC-5, 5637 and UMUC-3 cells were treated with pan/pan IR700/IR700 followed by cytotoxic amounts of NIR for each cell line. Around 20-minutes post NIR, the presence of cleaved caspase 3/7 was detected by addition of Caspase-Glo 3/7 reagent. None of the PIT treated cells resulted in cleaved caspase 3/7 levels above the baseline of untreated cells or cells not treated with NIR. Staurosporine was used as a positive control which generated a large excess of cleaved caspase 3/7 which was appropriately inhibited by the cell permeable, caspase-specific inhibitor Z-VAD-FMK.

C. Transmission electron microscopy confirms necrosis as a mode of cell death by pan IR700 based PIT. UMUC5 cells were incubated with pan IR700 (10μg/ml) for 60 minutes, followed by irradiation with no NIR (NIR 0 J/cm^2) (i) or NIR 4 J/cm^2 (ii). Twenty minutes post-NIR, both these cells were fixed for TEM in plate using 2.5% glutaraldehyde in 0.1M Cacodylate buffer, pH 7.4. The untreated cells in the left panel appear normal in size and morphology with intact plasma and nuclear membranes and organelles, whereas pan IR700 PIT treated cells appear larger in size, broken membranes, devoid of almost all cellular contents and surprisingly normal albeit swollen mitochondria.

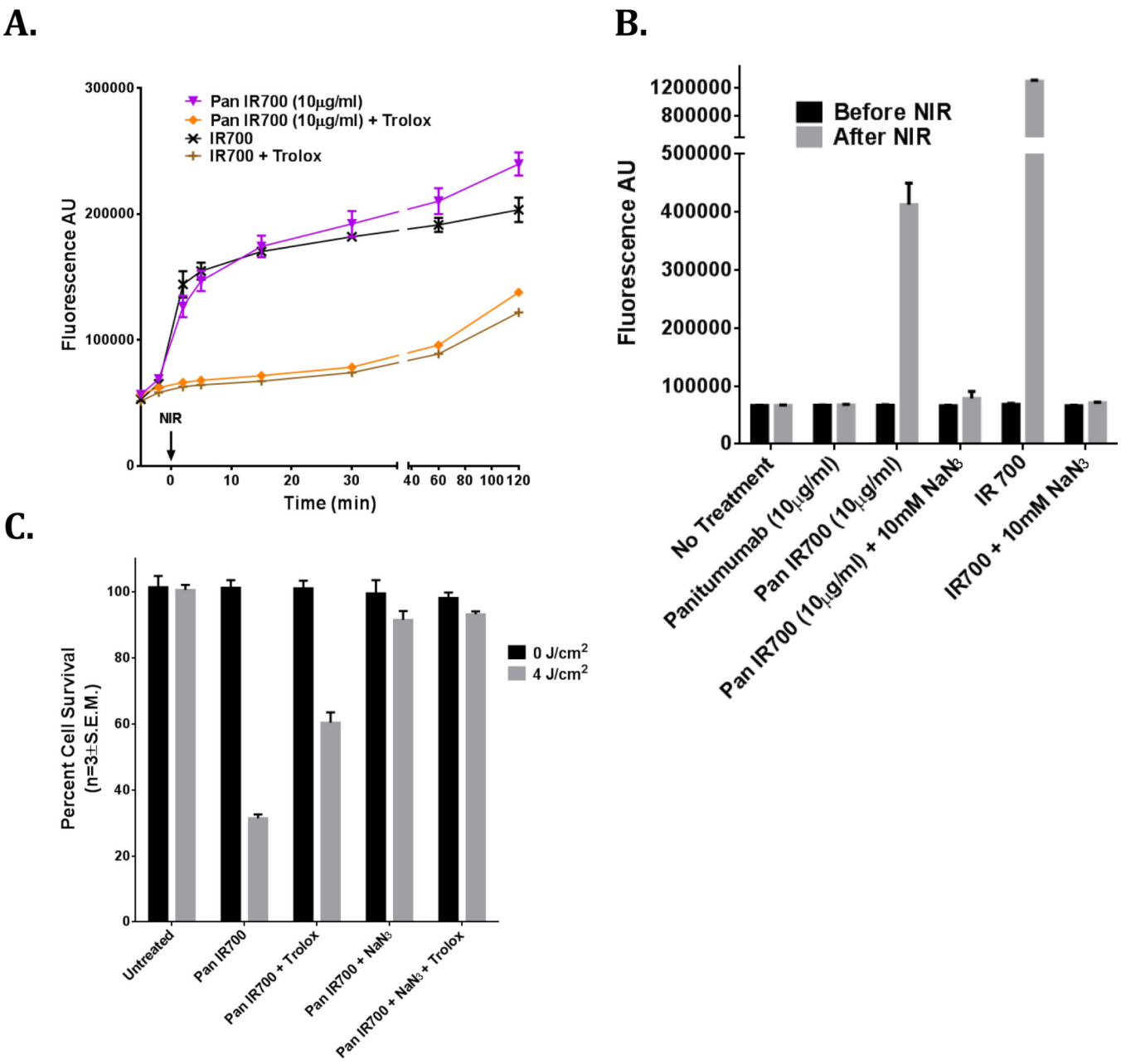

Figure 4. Contribution of oxygen free radicals to necrosis caused by pan IR700 based PIT

A. Pan IR700 and IR700 mediated PIT produces reactive oxygen species. UMUC5 cells pre-treated with DCFDA (20μM) were incubated with pan IR700 (10μg/ml) or an equivalent amount of IR700 with and without Trolox (1mM) followed by irradiation with NIR 4 J/cm^2 or no NIR (Supplemental Fig. 9). Immediately following NIR irradiation, production of ROS was measured as a function of DCA generation, a fluorescent substance with excitation maxima 488 nm and emission maxima 535 nm. There is an approximately three- to four-fold increase in the amount of ROS production in both pan IR700 and IR700 treated cells immediately after NIR treatment which is inhibited in the presence of Trolox.

B. Pan IR700 and IR700 mediated PIT produces singlet oxygen species. UMUC5 cells pre-treated with singlet oxygen sensor green were incubated with pan IR700 (10μg/ml) or an equivalent amount of IR700 with and without NaN_3 (10mM) followed by irradiation with NIR 4 J/cm^2. Immediately after NIR irradiation, the SOS production was measured at 535nm. There is an approximately four-fold increase in the amount of ROS production in both pan IR700 and IR700 treated cells immediately after NIR treatment which is quenched in the presence of NaN_3. In untreated cells or panitumumab treated cells, NIR exposure did not change SOS production compared to non NIR treated cells.

C. SOS quencher, NaN_3, protects the cells from pan IR700 PIT-induced cell death. UMUC5 cells were incubated with pan IR700 in the presence or absence of a ROS quencher (Trolox 1mM) or a SOS quencher (NaN_3, 10mM) or both followed by irradiation with no NIR or NIR 4J/cm^2. One hour later the resultant cell survival/death was measured using MTS reagent. The SOS quencher NaN_3 is able to completely rescue pan IR700 PIT induced cell death.

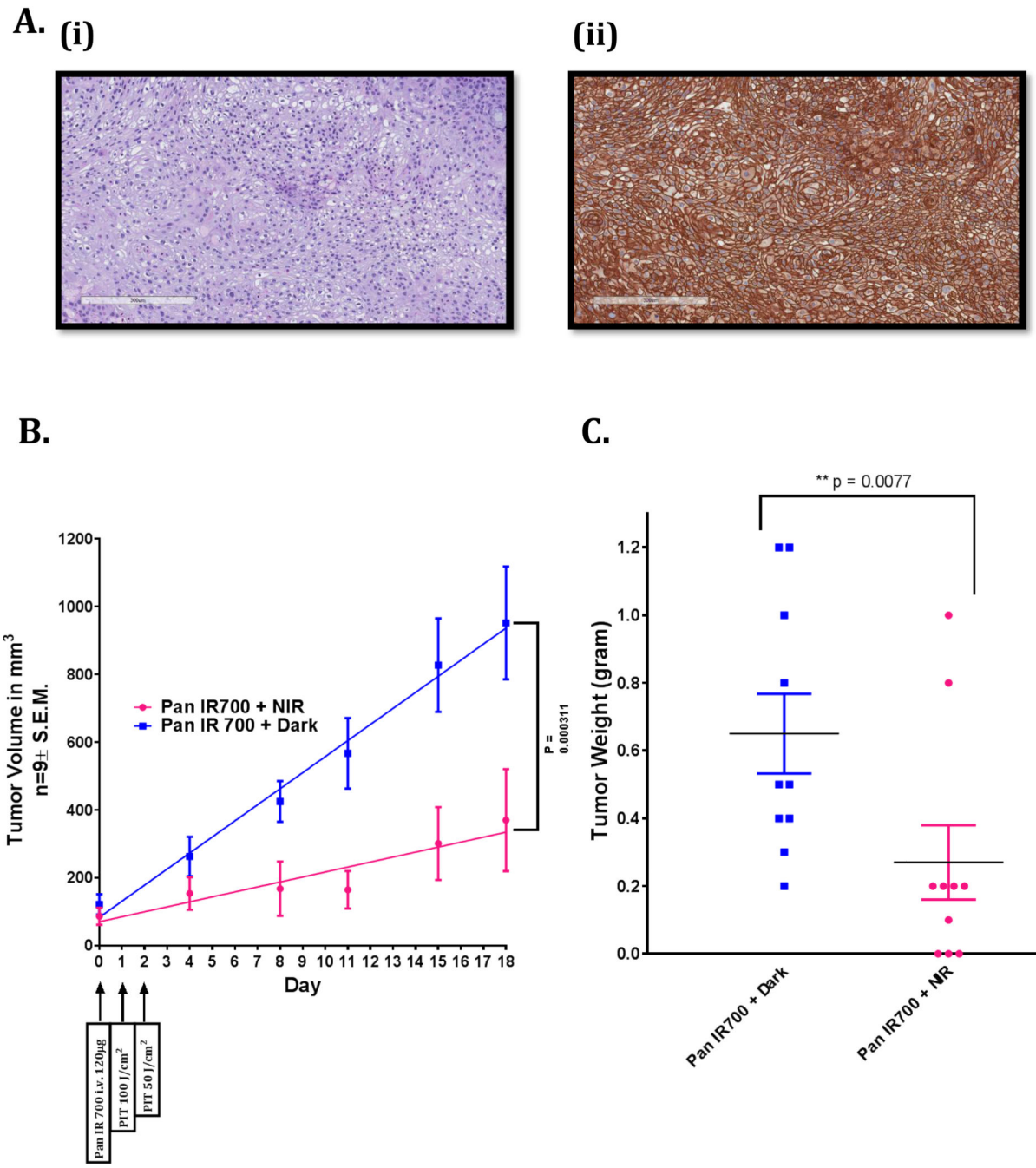

Figure 5. Effect of pan IR700 based PIT on UMUC5 xenograft

About 3 million cells (per animal) re-suspended in 100μl of Matrigel : PBS (1:1) were injected subcutaneously on the right thigh of female athymic nude mice. Tumors were measured two times a week using external calipers. Tumor volumes were calculated using a formula Tumor volume (mm^3) = Tumor length (mm) × Tumor breadth $(mm)^2$ × 0.5. After 7 days of injection of UMUC5 cells, tumors of volumes 50 – 100 mm^3 were seen in all the injected mice. The mice were randomized to groups of 10/treatment.

A. (i) H & E staining of UMUC5 xenograft showing morphology and (ii) Staining of hEGFR for UMUC5 xenografts shows very high expression of EGFR similar to UMUC5 cells *in vitro*.

B. Both groups of mice received 120μg of pan IR700/animal by i.v. injection. Control group (blue solid squares) did not receive any near IR radiation, whereas experimental mice (pink solid circles) received 100J/cm^2 and 50J/cm^2 NIR 24 hours and 48 hours post pan IR700 injection respectively. Tumor growth was attenuated in experimental mice (pan IR700 + NIR group).

C. At the end of the experiment the mice were euthanized and tumors were dissected out and weighted. Control group (blue solid squares) had significantly higher tumor weights (median – 0.5 g) than the experimental group (pink solid circles) (median weight – 0.2 g).